Ocular artifacts elimination from multivariate EEG signal using frequency-spatial filtering

Abhijit Bhattacharyya, Aarushi Verma, Radu Ranta, Ram Bilas Pachori

Ocular Artifacts Elimination from Multivariate EEG Signal using Frequency-Spatial Filtering

Abhijit Bhattacharyya, *Member IEEE*, Aarushi Verma, Radu Ranta, *Member IEEE*, Ram Bilas Pachori, *Senior Member IEEE*

Abstract

The electroencephalogram (EEG) signals record electrical activities generated by the brain cells and are used as a state-of-the-art diagnosis tool for various neural disorders. However, the unwanted artifacts often contaminate the recorded EEG signals and disturb the interpretation of the neuronal activity. This paper aims to propose an efficient automatic method to eliminate the ocular artifacts (OAs) from the multi-channel EEG signals with novel frequency-spatial filtering. The method combines dictionary-based spatial filtering and frequency based signal decomposition method, namely empirical wavelet transform (EWT). The artifact dictionary needed for spatial filtering is isolated from the raw data by (1) selecting the contaminated channels and (2) frequency-domain filtering. More precisely, the δ-rhythms of identified highly contaminated channels are selected and placed into an artifact dictionary. Afterward, the δ-rhythms of multi-channel EEG signals are spatially filtered using the built dictionary to seclude the OAs within a limited number of components. Further, the artifact components are eliminated and clean δ-rhythms are recovered using inverse spatial filtering technique. Finally, the clean δ-rhythms are combined with other EEG rhythms to reconstruct the OA-free signals. The proposed method is applied to OA contaminated synthetic and real multi-channel EEG signals with a convincing performance as compared to state of the art approaches. The proposed method removes the OAs without affecting the background EEG information. The proposed method can ease sensor signal interpretation and further processing, e.g. for BCI applications.

Index Terms

Electroencephalogram (EEG), ocular artifacts, spatial filtering, frequency-domain filtering, empirical wavelet transform (EWT).

I. Introduction

ELECTROENCEPHALOGRAM (EEG) is a non-invasive tool for measuring different neural activities of the brain [1]. Generally, EEG signal recording is carried out by placing the electrodes (from around 20 up to 256) on the scalp following the International 10-10 / 10-20 electrode positioning protocols [2]. EEG is extensively used in many research fields such as psychology, neuroscience, psychophysiology, and cognitive science. Apart from these, EEG also finds application in clinical research to identify and diagnose many brain pathology such as epilepsy [3], Alzheimers disease [4]. However, unwanted signals or artifacts from non-neuronal sources intertwine with EEG recordings, hindering EEG interpretation and may even result in misleading conclusions [5], [6]. The sources of artifacts can be either physiological (ocular, muscle, motion, cardiac) or non-physiological (electrode displacement, cables, equipment, stimulation) [7]. The ocular artifacts (OA) in the recorded EEG signal are attributed to the eye movements and blinks, which affect the electric field in the eyes and scalp surrounding regions [8]. More precisely, the OA appear due to voltage variations resulting from cornea-retina dipoles and eye-lid movements [9].

Regression algorithms underpin the simplest techniques for OA removal in the literature [10]. However these algorithms require reference electrooculography (EOG) channels to detect the artifacts [11]. Adaptive filtering is another approach for filtering the OA from EEG recordings. In this, the performance depends on selecting the reference signal used to estimate the artifact signal [12]. Adaptive filtering is suited for online implementation with no prior calibration, but the requirement of reference signal still exists [11]. The OA suppression based on blind source separation (BSS) estimates the sources of neural information and OAs without prior information of the mixing matrix. Once the sources are estimated, the artifactual sources can be removed [13]. Independent component analysis (ICA), a BSS technique, decomposes multichannel contaminated EEG data from different sources into independent components (ICs)[1]. The assumption is that the signals from different sources are independent and linearly mixed. OA-free sources are considered for the reconstruction of clean EEG data [13]. Different methods are proposed in the literature in order to identify artifact sources after ICA. In [15], the authors computed modified multiscale sample entropy (MMSE) and kurtosis for identifying ICA components with eye-blink artifacts that were further processed using wavelet thresholding to obtain clean EEG signals. One of the most known methods was introduced in [16], where authors proposed ICLabel classifier to categorise IC signals into brain, muscle, eye, heart, line noise, channel noise, and others. A supervised classification approach (combined with wavelet denoising) was also proposed by [17] for identifying

Abhijit Bhattacharyya and Aarushi Verma are with the Department of Electronics and Communication Engineering, National Institute of Technology Hamirpur, Hamirpur-177005, India, e-mail: abhijit@nith.ac.in.

Radu Ranta is with Universit de Lorraine, CNRS, CRAN, F-54000 Nancy, France.

Ram Bilas Pachori is with the Department of Electrical Engineering, Indian Institute of Technology Indore, Indore-453552, India

[1]Note that, using the algorithm in [14], a single-channel EEG can also be separated into the sources using ICA.

artifact sources. Still, even if automatic IC selection is indeed helpful in large scale studies and real-time applications such as BCI, these methods need training data to determine the model parameters and the quality of this data has significant impact on classifiers' ability to predict labels accurately. Note also that PCA can also be used for data decomposition. In [18], a comparative analysis is presented between ICA and principal component analysis (PCA) in removing EEG artifacts.

The assumption of orthogonality/independence is an important drawback for PCA/ICA methods, as it is not physiologically justified for brain sources (although acceptable for artifact sources). In [19] authors proposed artifact subspace reconstruction (ASR) for eliminating transient and large amplitude arifacts from multicannel EEG signals. Similar to PCA-based approaches, ASR reconstructs channel data from the remaining components after excluding large-variance components. The primary distinction is that ASR automatically identifies clean data segments and makes use of them as a benchmark to set thresholds for rejecting components [20].

Wavelet transform (WT) is another approach for filtering the OAs from EEG signals [21]. Authors in [22] showed that discrete wavelet transform (DWT) and stationary wavelet transform (SWT) applied to a single-channel EEG signal succeeds in filtering the artifacts. However, wavelet-approach ceases if spectral properties of artifact overlap with the spectral properties of EEG signals.

Various hybrid approaches have also been proposed in the literature for effective filtering of artifacts [17], [23]–[28]. Romo-Vazquez *et al.* [17] introduced an optimized automatic pipeline for artifact and noise cancellation combining BSS (SOBI), discriminant analysis (DA) and DWT based denoising. Akhtar *et al.* [23] proposed a multichannel OA removal technique combining spatially constrained ICA (SCICA) and wavelet denoising (WD) method. Peng *et al.* [24] combined DWT with adaptive noise cancellation (ANC) for OA removal. Their method overcomes the EOG reference signal's requirement as DWT is used to construct the OA reference signal. In [25], the authors proposed a single-channel OA filtering method by combining ANC with singular spectrum analysis (SSA). The SSA decomposition is used to estimate the reference signal for ANC. The performance of SSA-ANC is independent of the morphology of the OA, but it suffers from the problem of mode-mixing. In comparison to ICA, ANC requires more computation time but provides better performance in the portable environment [24]. In [26], empirical mode decomposition (EMD) and canonical correlation analysis (CCA) are combined for suppressing OA artifacts. Patel *et al.* [27] proposed an OA elimination technique in single-channel EEG by combining ensemble EMD (EEMD) and PCA methods. Authors in [28] use variational mode decomposition (VMD) and excluded the requirement of reference EOG signal to remove the OA from single-channel EEG. In [29], authors have employed local polynomial approximation based total variation (LPATV) technique to filter the OA from a single-channel EEG signal. Recently deep learning (DL) approaces have gained significant attention for EEG signal denoising. These models yield similar performance to those of conventional methods. However, the creation of DL solutions for EEG denoising necessitates the use of well-organized, standardised datasets with certain benchmarks. In [30] authors presented EEGdenoiseNet, a benchmark EEG dataset and quantified the performance of DL models for removal of various EEG artifacts.

The literature reveals that most OA filtering methods remove the OAs in single-channel EEG signals and tend to affect the background EEG signals while cleaning the artifacts. Delta band being the highly contaminated rhythm from OAs [25], is severely affected in the filtering process, leading to loss of useful EEG information. This paper proposes a new hybrid approach combining frequency and spatial filtering techniques to filter the OAs from multichannel EEG signals, preserving the necessary EEG information. The method combines the subspace correlation approach (SCA) [31] with frequency domain filtering techniques, namely, empirical wavelet transform (EWT) [32]. The proposed method does not use additional signals as reference for the artifacts (e.g. EOG), but instead extracts a basis of the artifact space directly from the raw data. The performances of the method are assessed in both synthetic and real multichannel EEG signals contaminated with OAs. Our method's performance is compared with the combination of ICA and EWT based frequency domain filtering and also with the EWT-based monochannel method for OA removal. The proposed method eliminated the OAs from multichannel EEG recordings with minimal loss of background signal information.

The rest of the paper has following sections: Section II describes the multichannel simulated and real EEG datasets used in this work. Section III explains the methodology used for multichannel OA elimination; Section IV presents the experimental results with a discussion on the effectiveness of the proposed filtering technique. Section V contains the conclusion.

II. Simulated and real EEG Datasets

A. Simulated EEG dataset

The semi-simulated dataset [33] contains the EEG recordings from 27 healthy subjects, which were contaminated manually with OAs. This work randomly considers total 30 EEG signals of 30-second duration, recorded using 19 electrodes, following the 1020 International electrode system standard. For generating the OA contaminated signals, these clean signals were artificially contaminated with the EOG signals from the same subjects following the model:

$$\text{EEG}^{s,e}_{\text{contaminated}} = \text{EEG}^{s,e}_{\text{clean}} + M_e\text{VEOG} + N_e\text{HEOG}. \tag{1}$$

The VEOG stands for vertical-EOG, which is the difference between upper and lower EOG electrode signals. Similarly, HEOG represents horizontal-EOG, which is the difference between left and right EOG electrode signals. M_e and N_e are the VEOG

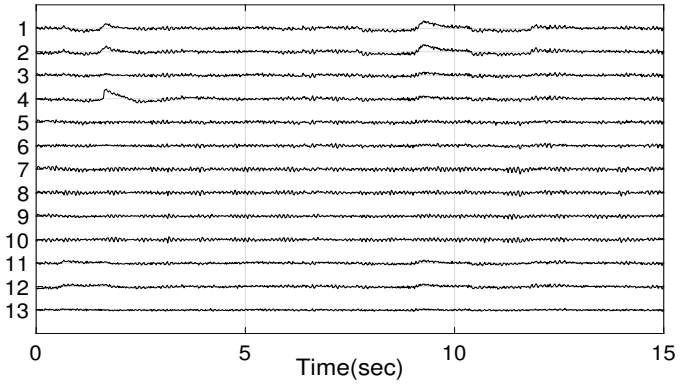

Fig. 1. Plot of OA contaminated simulated multichannel EEG signal.

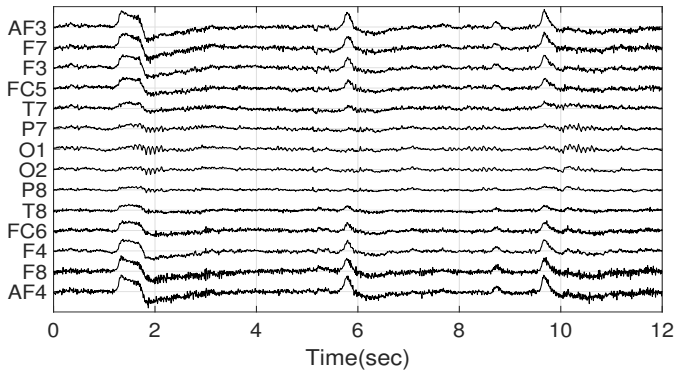

Fig. 2. Plot of multichannel real EEG signal contaminated with OAs.

and HEOG contamination coefficients (scaling factors), respectively, where e represents the electrode number. The index s represents the subject number. They are used for having different amplitudes for the artifacts on different channels. Each EEG signal was sampled at 200 samples per second. Fig. 1 shows the first 13 channels of an OA contaminated sample EEG recording.

B. Real EEG dataset

The EEG motor movement/imagery dataset [34] provided by Physionet [35] is considered for evaluation of the proposed method. The 10-20 international electrode standard was followed for placing 64 electrodes on the scalp of 109 volunteers to obtain over 1500 recordings. Each EEG recording containing 64 EEG channels is of one or two minutes duration and sampled at 160 Hz. We have randomly selected 30 EEG recordings for evaluation of the proposed method. An example of a real OA contaminated multichannel EEG signal is shown in Fig. 2. Based on bibliography [25], OAs lead to high energy of delta waves. This is also confirmed by the analysis of our data (see Fig. 3 for brain topographies), which shows that high amplitude delta rhythms are mainly present in the frontal areas, i.e. on the electrodes close to the eyes.

III. Methods

The flow diagram of the proposed OA elimination method is presented in Fig. 4. It can be seen that EWT based frequency-domain filtering decomposes the OA contaminated multi-channel EEG signal into rhythms (δ, θ, α, β, and γ) [36]. Even if OAs mostly contaminate the δ rhythms of frontal electrodes (see Fig. 3), not all of them are necessarily corrupted, so we computed energy ratios (ERs) for δ rhythms to identify the contaminated channels (see eq. 22). This yields an artifact dictionary which comprises the δ rhythms of the contaminated channels with high ER values. In the next step, a common subspace of the built dictionary and the δ-rhythms of the multichannel EEG signal is found by rotating their respective basis matrices one onto the other using the SCA method. After rotation, the OAs and neural activities become spatially separated. The artifact containing components isolated by SCA are eliminated using a diagonal gain matrix followed by inverse spatial filtering for recovering the clean δ-rhythms of the multichannel EEG signal. Finally, the cleaned δ rhythms are combined with the remaining rhythms for obtaining OA-free multichannel EEG signal. The following subsections describe the proposed methods in detail and present the OA filtering pipeline employed in this work.

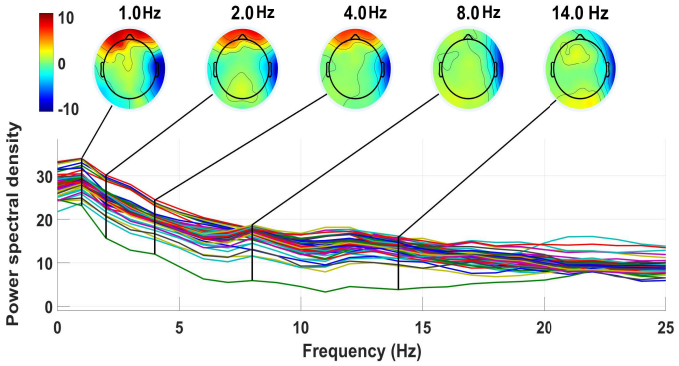

Fig. 3. Plots of PSDs of all the real EEG channels and brain topographical maps.

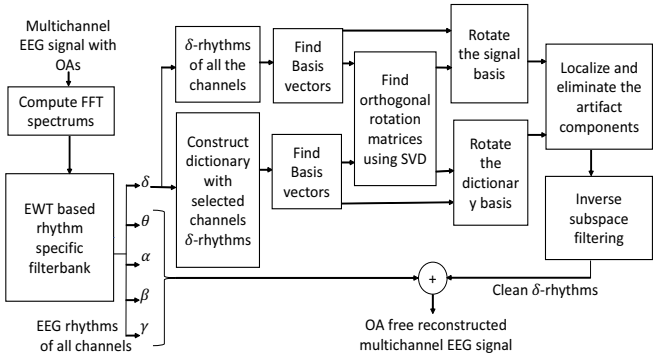

Fig. 4. Flow diagram of the proposed multivariate OA elimination method using frequency-spatial filtering.

A. Empirical Wavelet Transform

EWT [32] decomposes non-stationary signals into multiple subbands, belonging to different oscillatory levels. This is carried out by creating an adaptive wavelet-based filter bank. The steps involved in EWT are summarised as follows: (i) Obtaining the signal spectrum using Fast Fourier Transform (FFT) in the range 0 to π (ii) Applying boundary detection techniques to segment the Fourier spectrum as per the spectral information content (iii) Using the concept of LittlewoodPaley and Meyer wavelets [37], to define empirical wavelets as bandpass filters on each segment. The scaling function and the wavelet function are mathematically expressed as,

$$\phi_i(\omega) = \begin{cases} 1 & ,|\omega| \leq \omega_i - \tau_i \\ \cos(z_i) & ,\omega_i - \tau_i \leq |\omega| \leq \omega_i + \tau_i \\ 0 & ,\text{otherwise} \end{cases} \tag{2}$$

and

$$\psi_i(\omega) = \begin{cases} 1 & ,\omega_i + \tau_i \leq |\omega| \leq \omega_{i+1} - \tau_{i+1} \\ \cos(z_{i+1}) & ,\omega_{i+1} - \tau_{i+1} \leq |\omega| \leq \omega_{i+1} + \tau_{i+1} \\ \sin(z_i) & ,\omega_i - \tau_i \leq |\omega| \leq \omega_i + \tau_i \\ 0 & ,\text{otherwise} \end{cases} \tag{3}$$

where

$$z_i = \frac{\pi}{2}\rho(\omega_i, \tau_i) = \frac{\pi}{2}\rho(\frac{1}{2\tau_i}(|\omega| - \omega_i + \tau_i)] \tag{4}$$

such that

$$\rho(r) = \begin{cases} 0 & ,r \leq 0 \\ 1 & ,r \geq 1 \end{cases} \quad \text{and } \rho(r) + \rho(1-r) = 1 \quad \forall r \in [0,1] \tag{5}$$

and $2\tau_i$ is the width of transition phase centered around each boundary frequency, ω_i. By proper selection of σ ($\tau_i = \sigma\omega_i, 0 < \sigma < 1$) tight frame of empirical wavelets are obtained. It has been proved in [32] that σ following the condition in equation (6) provides tight frame.

$$\sigma < \min_i \left(\frac{\omega_{i+1} - \omega_i}{\omega_{i+1} + \omega_i} \right) \tag{6}$$

Therefore, equations (2) and (3) can be expressed in the form of equations (7) and (8), respectively.

$$\phi_i(\omega) = \begin{cases} 1 & \text{if } |\omega| \leq (1-\sigma)\omega_i \\ \cos(z_i) & \text{if } (1-\sigma)\omega_i \leq |\omega| \leq (1+\sigma)\omega_i \\ 0 & \text{otherwise} \end{cases} \tag{7}$$

and

$$\psi_i(\omega) = \begin{cases} 1 & , (1+\sigma)\omega_i \leq |\omega| \leq (1-\sigma)\omega_{i+1} \\ \cos(z_{i+1}) & , (1-\sigma)\omega_{i+1} \leq |\omega| \leq (1+\sigma)\omega_{i+1} \\ \sin(z_i) & , (1-\sigma)\omega_i \leq |\omega| \leq (1+\sigma)\omega_i \\ 0 & , \text{otherwise} \end{cases} \tag{8}$$

where z_i now expressed as,

$$z_i = \frac{\pi}{2}\rho(\omega_i, \sigma) = \left[\frac{\pi}{2}\rho\left(\frac{1}{2\sigma\omega_i}\left(|\omega| - (1-\sigma)\omega_i\right)\right)\right] \tag{9}$$

The inner product of the signal with the empirical wavelet function and scaling function provides the detail and approximation coefficients, respectively.

B. Spatial Filtering

The multichannel OA contaminated EEG signals can be expressed as a linear mixture model (1). In this context, spatial filtering techniques can be effectively applied to isolate the OAs into one or very few number of components/sources. Spatial filtering techniques have been frequently used for various EEG artifact cancellation [38]. The underlying idea of spatial filtering is to separate the raw signal space (the set of all signals that can be generated through all arbitrary full rank linear transforms applied to the actual recordings) into various subspaces specific to different activities, in this work OAs (artifact space) and neural activity (clean signal space). One can only take into account the basis of the subspace specific to brain activity when reconstructing the clean EEG signal after separating the two subspaces (artifact and clean signal space) and thus their bases. In our work, we complement EWT based monochannel filtering with different spatial filtering techniques, inspired either from subspace based methods [31] or from BSS methods [39].

1) Subspace Correlation Approach (SCA): The SCA can be described by the following steps:

In the first step, a basis for the signal space has been found by whitening. The basis $\mathbf{Z}$ for the multichannel signal $\mathbf{S}$ (samples by channels, $N \times C$) can be obtained after eigen decomposition of scatter/covariance matrix $\mathbf{T_S}$.

$$\mathbf{T_S} = \mathbf{S^T S} = \mathbf{W D W^T} \tag{10}$$

$$\mathbf{Z} = \mathbf{S W D^{-\frac{1}{2}}} \tag{11}$$

where $\mathbf{W}$ and $\mathbf{D}$ are the eigenvector and eigenvalue matrices of the covariance matrix $\mathbf{T_S}$. The rotation of basis $\mathbf{Z}$ by right multiplying a specified orthogonal matrix $\mathbf{P}$ will make the subspaces for artifacts and physiological activities as orthogonal as possible. Therefore, the next step is to derive the desired orthogonal matrix $\mathbf{P}$, optimized for our objective. Note that the whitening step is common for the ICA based methods also (see below), the main difference being that in ICA the $\mathbf{P}$ matrix is found by optimizing a different criterion, namely statistical independence.

In the second step, a second dataset $\mathbf{A}$ has been constructed with the filtered versions (δ-rhythms) of the one or few identified contaminated EEG channels, which can be considered as artifact dictionary. The inclusion of more than one filtered channel helps to bring the variability in the artifact characteristics. The basis $\mathbf{Z_a}$ of the dictionary space can be found using whitening:

$$\mathbf{Z_a} = \mathbf{A W_a D_a^{-\frac{1}{2}}} \tag{12}$$

In the third step, a common subspace between the signal $\mathbf{S}$ and dictionary $\mathbf{A}$ have been derived by rotating the two bases $\mathbf{Z_a}$ and $\mathbf{Z}$ onto each other, as proposed in [31]:

i) Performing the singular value decomposition (SVD) of the matrix $\mathbf{C} = \mathbf{Z^T Z_a}$

$$\mathbf{C} = \mathbf{P \Sigma R^T} \tag{13}$$

ii) Considering $\mathbf{P}$ and $\mathbf{R}$ as the desired rotation matrices for rotating the basis $\mathbf{Z}$ and $\mathbf{Z_a}$ respectively.

$$\mathbf{Y} = \mathbf{ZP} = \mathbf{S W D^{-\frac{1}{2}} P} \tag{14}$$

$$\mathbf{Y_a} = \mathbf{Z_a R} = \mathbf{A W_a D_a^{-\frac{1}{2}} R} \tag{15}$$

The constructed spatial filters $\mathbf{V}$ and $\mathbf{V_a}$ can be expressed as,

$$\mathbf{V} = \mathbf{W D^{-\frac{1}{2}} P} \tag{16}$$

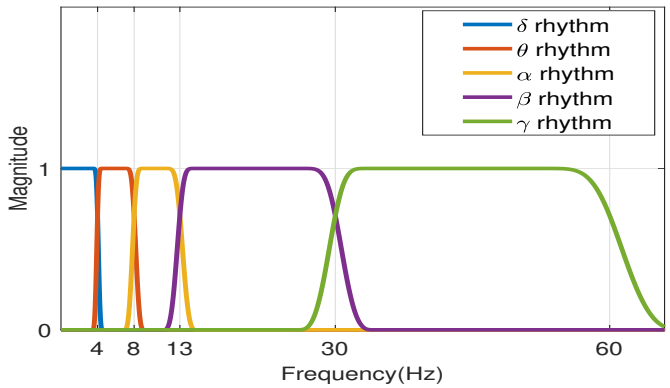

Fig. 5. Plot of EWT based fixed boundary filter bank for decomposing the EEG channels into rhythms.

$$\mathbf{V_a} = \mathbf{W_a} \mathbf{D_a}^{-\frac{1}{2}} \mathbf{R} \tag{17}$$

Finally, the rotated basis $\mathbf{Y}$ and $\mathbf{Y_a}$ can be expressed as,

$$\mathbf{Y} = \mathbf{S}\mathbf{V} \tag{18}$$

$$\mathbf{Y_a} = \mathbf{A}\mathbf{V_a} \tag{19}$$

One can verify that signal space and dictionary space $\mathbf{Y}$ and $\mathbf{Y_a}$ have become aligned:

$$\mathbf{Y^T Y_a} = \mathbf{\Sigma} \tag{20}$$

The common subspace basis between the signal and dictionary can be identified by the singular values in $\mathbf{\Sigma}$, which are close to 1. The obtained components $\mathbf{Y} = \mathbf{SV}$ after spatial filtering will be arranged starting with common basis vectors (i.e., OA components) of $\mathbf{S}$ and $\mathbf{A}$. In contrast, uncommon physiological basis vectors will be present at last. Afterward, the OA-free multichannel signal $\overline{\mathbf{S}}$ can be recomposed as follows:

$$\overline{\mathbf{S}} = \mathbf{SVGV^{-1}} = \mathbf{YGV^{-1}} \tag{21}$$

where $\mathbf{G} = \mathbf{diag}(\mathbf{0}, \ldots, \mathbf{0},\ \mathbf{1}, \ldots \mathbf{1})$ is the diagonal gain matrix for retaining the desired components only.

2) Blind source separation: BSS method demixes multidimensional signals into components/sources as independent as possible from each other. There is no or very little prior knowledge about the mixing matrix. Therefore, the aim is to separate a mixture into its source components without knowing the mixing process. BSS methods have been proven useful in removing artifacts from EEG signals [13]. The famous BSS algorithms in the literature are either based on ICA [40] or on second-order statistics (SOS) [41] or on the combination of both ICA and SOS [42]. The BSS methods can be employed for extracting the OA sources without the knowledge of mixing coefficients if the hypothesis of independence of OA patterns and brain sources is followed. Different ICA methods can be used for separating the artifact components. We propose here to use EFICA [42] for two main reasons: (1) it is derived from the well known computationally efficient and performant FastICA and (2) it adapts to the data (adaptive nonlinearity).

C. Proposed OA Filtering Pipeline

It should be noted that frequency-based filtering and spatial filtering can standalone filter the OAs and recover neural information. However, the fact is that not all channels are contaminated with OAs, which drives us to combine spatial filtering with frequency-based filtering to develop a procedure that requires eliminating only fewer components (only the contaminated ones) and thus reducing the computational burden. This section describes the proposed framework for combining these two techniques and presents a novel methodology for OA removal.

*1) **EWT based EEG rhythm separation**:* The OAs severely contaminate the δ-rhythms of EEG signals, requiring traditional band-specific filtering for their removal. The EWT decomposes signals after determining adaptive boundary frequencies in the signal spectrum. However, such decomposition does not guarantee the extraction of traditional bands (i.e., rhythms in the case of EEG). Moreover, extraction of subbands adaptively may result in the presence of OAs in multiple narrowband low frequency subband signals, necessitate extensive processing, and be ineffective. The frequency-domain filtering can decompose EEG signals into rhythms (traditional bands), namely δ, θ, α, β, and γ specified by the frequency range of 04, 48, 813, 1330, 3060 Hz, respectively. The separation of EEG rhythms using EWT was proposed in [36], where prior boundary/edge frequencies $\{\omega_i\}_{i=1,2\ldots,5}$ are set to 4 Hz, 8 Hz, 13 Hz, 30 Hz, 60 Hz, respectively for segmenting the Fourier spectrum in the range $[0, f_s/2]$. Fig. 5 depicts the EWT filterbank generated for decomposition of EEG signal into rhythms. One can see

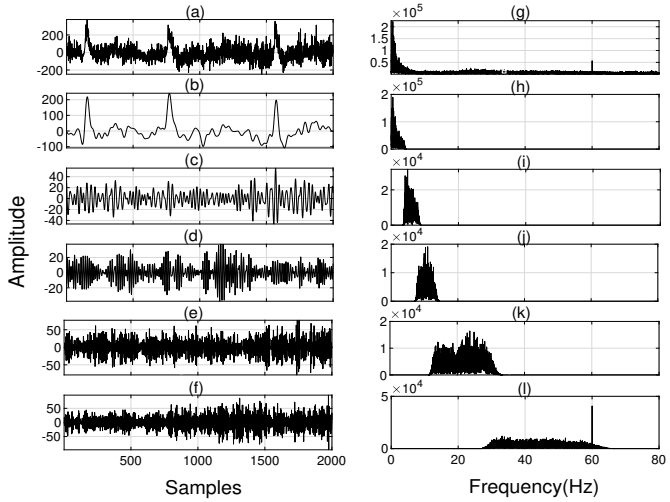

Fig. 6. The left column ((a) to (f)) from top to bottom shows EEG signal with OAs and its rhythms δ, θ, α, β, and γ obtained using an EWT-based filter bank. The right column ((g) to (l)) shows their corresponding frequency spectrums.

that the filter bank generated by EWT has small transition bands with almost negligible stop-band and pass-band ripples. The obtained EEG rhythms and their corresponding spectrums using EWT are shown in Fig. 6. In the subsequent step, the extracted δ-rhythms are spatially filtered without altering the remaining bands.

Algorithm 1: Proposed EWT-SCA filtering approach.

Input: Multivariate EEG signal intermixed with ocular artifacts, $y(n)$.
Output: Multivariate clean EEG signal, $\tilde{y}(n)$.
Step 1: Develop EWT based filterbank with EEG rhythm specific boundary frequencies using equations (7) and (8).
Step 2: Decompose every channel into rhythms δ, θ, α, β, and γ; create the first dataset $\mathbf{S}$ with the δ-rhythms of all the channels.
Step 3: Identify contaminated EEG channels with high ER_{δ_i} values using equation (22) and create the artifact dictionary $\mathbf{A}$ with the δ-rhythms of the highest contaminated EEG channels from different spatial locations.
Step 4: Compute the bases $\mathbf{Z}$ and $\mathbf{Z_a}$ for the matrices $\mathbf{S}$ and $\mathbf{A}$ using equations (11) and (12), respectively.
Step 5: Find the desired rotation matrices $\mathbf{P}$ and $\mathbf{R}$ with SVD of the matrix $\mathbf{C}$ using equation (13).
Step 6: Construct the spatial filters $\mathbf{V}$ and $\mathbf{V_a}$, and rotate the matrices $\mathbf{S}$ and $\mathbf{A}$ using equations (18) and (19), respectively.
Step 7: Obtain the OA-free matrix $\overline{\mathbf{S}}$ by suppressing the contaminated components using equation (21).
Step 8: Finally recover the clean multivariate EEG signal $\tilde{y}(n)$ by combining the matrix $\overline{\mathbf{S}}$ representing clean δ-rhythms with other EEG rhythms extracted in Step 2.

*2) **Multichannel OA suppression**:* As stated earlier, spatial filtering techniques complement the EWT based frequency-domain filtering, extending OA suppression method for multichannel signals. We use SCA as a primary spatial filtering technique, and also employ different flavours of BSS techniques for comparison purpose.

SCA based spatial filtering: In our research, SCA spatially separates the OAs from the neural activities (i.e., δ component of OA contaminated multichannel EEG signal) using an artifact dictionary.

The OAs propagate through the brain and are projected linearly onto the different channels (have distinct spatial locations) with different contamination coefficients. Further, some artifacts appeared differently on different channels because their (dipolar) sources had different orientations (e.g. eye blinks and eye movements). Due to this various artifact patterns were observed on different channels. Therefore, an artifact-rich dictionary was formed by including highly contaminated EEG channels from different spatial locations of the scalp. For identifying the channels with high contamination, various approaches were used (such as selecting channels with high energy, with high δ-rhythm energy, channels have a high correlation with the δ-rhythm of highest energy channel, and channels with high ER values). The ER of δ-rhythm approach provided the best results and is adapted here. The ER corresponding to δ-rhythm of each channel of the multichannel EEG signal (contaminated) can be computed as,

$$\mathrm{ER}_{\delta_i} = \frac{E_{\delta_i}}{E_{\delta_i} + E_{\theta_i} + E_{\alpha_i} + E_{\beta_i} + E_{\gamma_i}} \tag{22}$$

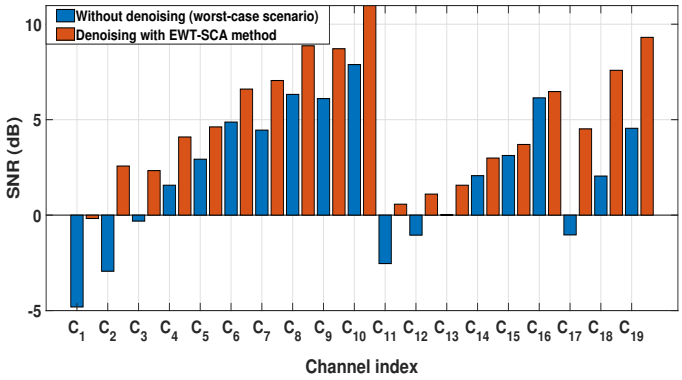

Fig. 7. Plot of SNRs of individual channel before and after OA removal.

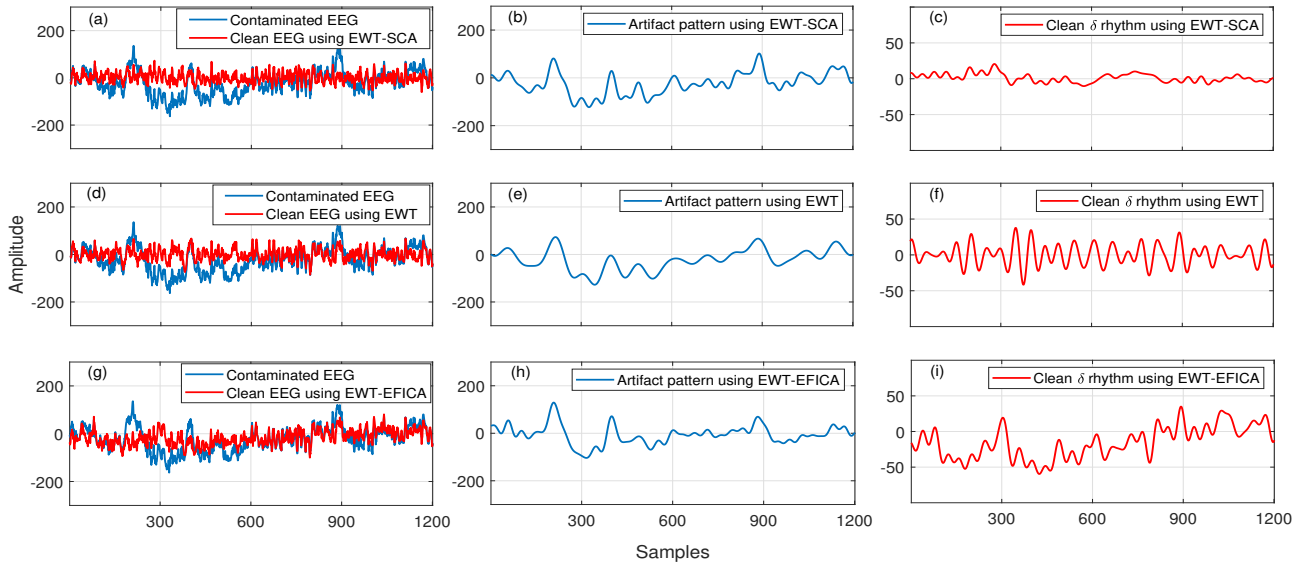

Fig. 8. Plots of the OA contaminated EEG signals overlapped with clean EEG signals (left column: (a), (d), and (g)), artifact patterns (middle column: (b), (e), and (h)), and recovered clean δ-rhythms (right column: (c), (f), and (i)).

where, $E_{\delta_i}, E_{\theta_i}, E_{\alpha_i}, E_{\beta_i}, E_{\gamma_i}$ are the energies of $\delta, \theta, \alpha, \beta$ and γ rhythms, respectively for the ith channel of the contaminated multichannel EEG signal. The proposed method uses the raw EEG data to automatically determine the value of k (number of selected dictionary channels). The value of k is determined based on the set threshold of ER_δ. For a raw EEG data $y(n)$, the channels with ER_δ values greater than $\mu_{y_\delta} + \text{Th} * \sigma_{y_\delta}$ will be included in the dictionary. The parameters μ_{y_δ} and σ_{y_δ} denote the mean and standard deviation (STD) of the ER_δ values across all channels of the raw EEG signal y. The variable Th denotes the threshold value. The δ-rhythms of the k selected channels form the dictionary of artifacts.

ICA based spatial filtering: ICA estimates the sources of neural information in multichannel EEG signals. Following a similar approach, the idea is to apply ICA on the delta rhythm and detect the artifact sources followed by their elimination. The primary challenge in ICA based decomposition is identifying artifact components/sources that are carried out following the high energy criteria (i.e., OA sources assumed to have higher energy than neural sources).

It should be noted that ICA performs spatial filtering without any dictionary or second dataset, unlike SCA. However, contrary to ICA, SCA components are naturally ordered from OA sources at the top followed by the neural sources; hence no effort is required to detect the artifact components. After the spatial filtering, the artifact components are discarded, and clean δ-rhythms are recomposed, further combined with other EEG rhythms to recover the clean multichannel EEG signals. The step-by-step procedure of EWT-SCA method for ocular artifact removal is represented using Algorithm 1.

D. Performance Measures

The proposed frequency-spatial filtering method's effectiveness in removing the OAs from the multichannel EEG signal is validated using the following three different performance measures:

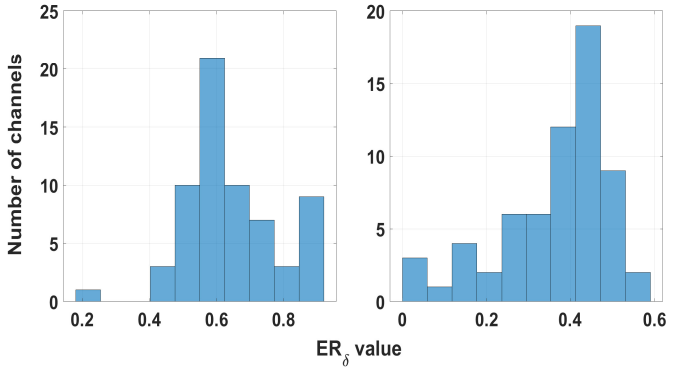

Fig. 9. Plots of the histograms of the ER$_\delta$ values for raw (left) and OA-removed (right) multichannel real EEG signals.

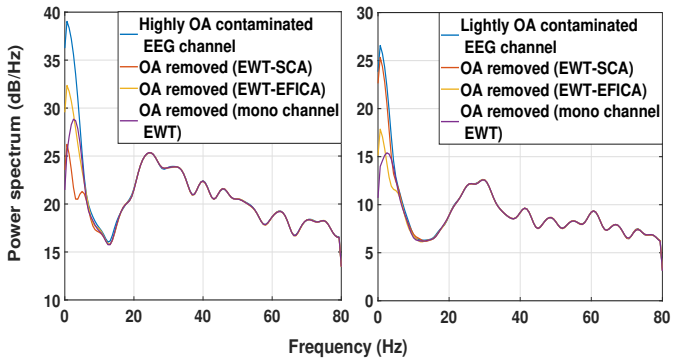

Fig. 10. Plots of the PSDs of OA contaminated and clean EEG signals considering highly (AF7) and slightly (T10) contaminated channels.

1) ***Percentage change in ER****:* The Percentage channge in ER (PCER) measures the reduction of artifact in the δ rhythm after applying the proposed method, which is mathematically expressed as,

$$\Delta ER_{\delta_i} = (ER_{\delta_i} - \overline{ER}_{\delta_i}) \times 100\% \tag{23}$$

where ER_{δ_i} is the ER corresponding to δ-rhythm of i^{th} contaminated channel as described in (22).
Similarly, $\overline{ER}_{\delta_i}$ denotes the ER corresponding to δ- rhythm of the cleaned i^{th} EEG channel, expressed as

$$\overline{ER}_{\delta_i} = \frac{\overline{E}_{\delta_i}}{\overline{E}_{\delta_i} + \overline{E}_{\theta_i} + \overline{E}_{\alpha_i} + \overline{E}_{\beta_i} + \overline{E}_{\gamma_i}} \tag{24}$$

where, $\overline{E}_{\delta_i}, \overline{E}_{\theta_i}, \overline{E}_{\alpha_i}, \overline{E}_{\beta_i}, \overline{E}_{\gamma_i}$ are the energies of $\delta, \theta, \alpha, \beta$ and γ rhythms, respectively for the i^{th} channel of the cleaned multichannel EEG signal.

2) ***Average mean absolute error (MAE) in power spectral density (PSD) values****:* To measure the proficiency of the proposed method in preserving the neural content while removing OAs, MAE in PSD values are computed. In the PSD of i^{th} channel, the MAE corresponding to rhythm $r \in \{\theta,\ \alpha,\ \beta,\ \gamma\}$ can be computed as [25],

$$MAE_{PSD}^{r_i} = \frac{\sum_{k=K_1}^{K_2} \mid \overline{PSD}_{r_i}(k) - PSD_{r_i}(k) \mid}{K_2 - K_1} \tag{25}$$

where K_1 and K_2 denote frequency bins of the PSD of tainted, ($PSD_{r_i}(k)$) and cleaned ($\overline{PSD}_{r_i}(k)$) rhythms of the i^{th} channel EEG record.
Finally, the average MAE (AMEA) in PSD values can be computed

$$AverageMAE_{PSD}^{r} = \frac{1}{M}\sum_{i=1}^{M} MAE_{PSD}^{r_i} \tag{26}$$

where M denotes the total number of EEG channels.

*3) **Signal to noise ratio (SNR)**:* To evaluate the effectiveness of the signal reconstruction, SNR values are computed before and after the OA artifacts are removed. However, since the clean EEG signals are also available, the SNR computation is only done for simulated EEG recordings. The SNR for subject s and electrode e at the input (i/p) and output (o/p) of the proposed method are defined as,

$$\text{SNR}_{\text{i/p}}^{s,e} = 10\log_{10}\left(\frac{\text{rms}(\text{EEG}_{\text{clean}}^{s,e})}{\text{rms}(M_e\text{VEOG} + N_e\text{HEOG})}\right) \tag{27}$$

$$\text{SNR}_{\text{o/p}}^{s,e} = 10\log_{10}\left(\frac{\text{rms}(\text{EEG}_{\text{reconstructed}}^{s,e})}{\text{rms}(\text{EEG}_{\text{clean}}^{s,e} - \text{EEG}_{\text{reconstructed}}^{s,e})}\right) \tag{28}$$

The mixing coefficients M_e and N_e are defined in eqn (1). The average SNR (ASNR) for a given session is then determined using the average of the channel-wise SNR readings.

IV. Experimental Results

This section presents the performance of the proposed combinations of frequency and spatial filtering techniques (namely EWT-SCA, FIR-SCA, EWT-EFICA, FIR-EFICA). However, only the outcomes of the best-performing methods, such as EWT-SCA, EWT-EFICA, and monochannel EWT, are exhibited and discussed next. The performance of the EWT-SCA method on OA contaminated simulated multichannel EEG signals is presented in Table I. The method's performance is exhibited in terms of the maximum obtained PCER of δ rhythm, AMAE in PSD for remaining rhythms, and ASNR measures. It can be seen in Table I that the proposed method has achieved high values of maximum PCER for δ rhythms for almost all the simulated sessions. These obtained values substantiate that EWT-SCA removes the OAs from δ-rhythms of multichannel EEG signals. On the other hand, the low values of AMAE in PSD in other rhythms indicate that the method works well in preserving neural information. After the OAs from multichannel EEG signals were removed, the proposed method provided better ASNR values. Fig. 7 shows the improvement in channel-wise SNR for a considered EEG record.

Table II presents the performance of the EWT-SCA method in removing OAs from real multichannel EEG signals. The obtained maximum PCER for δ-rhythms and AMAE in PSD values reveal the effectiveness of OA removal in real EEG signals.

The performance of the EWT-EFICA method in removing OAs from real multichannel EEG signals is exhibited in Table III. We have evaluated EWT-EFICA method on all the considered real EEG sessions. However, the best five results are presented in the table. The global mean and STD values considering all the real EEG sessions are 55.082 $\pm$ 6.6457, 10.7879 $\pm$ 6.5029, 1.61E-14 $\pm$ 6.59E-15, 1.09E-14 $\pm$ 5.30E-15, 6.83E-15 $\pm$ 5.47E-15 corresponding to maximum ΔER_δ, AMAE_θ, AMAE_α, AMAE_β, and AMAE_γ, respectively. It can be observed in the table that the obtained maximum PCER values for δ rhythms are significantly lower than the corresponding values obtained using the EWT-SCA method. Thus, the maximum PCER values indicate the presence of OAs even after applying the EWT-EFICA method. After using EWT-EFICA, OAs spread across a substantial number of independent components (ICs), making it challenging to distinguish between clean signal space and artifact space. Also, the high AMAE in PSD values for θ-rhythms clearly states the undesired alteration of neural information after artifact removal. Table IV depicts the obtained results when EWT is standalone applied (cutoff frequency 2 Hz) channel by channel on real OA contaminated EEG records. The global mean and STD values of the monochannel EWT considering all the real EEG sessions are 49.07 $\pm$ 7.236, 1.31E-14 $\pm$ 8.99E-15, 7.55E-15 $\pm$ 5.044E-15, 4.84E-15 $\pm$ 5.67E-15, 2.91E-15 $\pm$ 4.99E-15 for maximum ΔER_δ, AMAE_θ, AMAE_α, AMAE_β, and AMAE_γ, respectively. It can be noticed that though neural information is preserved in θ, α, β, and γ rhythms, the obtained maximum PCER values of δ rhythms are significantly lower compared to EWT-SCA and EWT-EFICA methods. The lower PCERs can be attributed to the set cutoff frequency (2 Hz) of monochannel EWT. The PCER may be increased by raising the cutoff frequency, but at the expense of losing delta band information.

Fig. 8 presents a real OA contaminated EEG signal, its clean versions, OA-free δ-rhythms, and the extracted artifact patterns obtained using EWT-SCA, monochannel EWT, and EWT-EFICA methods. It can be observed that the EWT-EFICA method fails to remove the low-frequency baseline component of the signal.

The starting hypothesis is that channels with high ER of δ-rhythm represent OA contaminated signals. These channels are selected as explained previously (see eq. (22) and following paragraph). In our experiments, the value of the threshold Th has been empirically set as 1.8. However, a 10% change in the threshold value has no appreciable impact on the method's performance. It is noteworthy that in the absence of eye artifacts k will be automatically set to zero and the process won't be continued. The histogram plots in Fig. 9 show that for the cleaned multichannel EEG signal $\tilde{y}(n)$, none of the channels have an ER_δ value greater than the $\mu_{\tilde{y}_\delta} + \text{Th} * \sigma_{\tilde{y}_\delta}$, so k is set to zero. The experiments have also shown that EWT-SCA-based processing of clean/lightly OA-affected EEG recordings results in a minimal alteration in the signals' delta bands as demonstrated in Fig. 10.

The figure presents PSD plots for OA contaminated and clean EEG signals considering both highly and slightly affected channels for a real EEG record. It is clear that for each of the scenarios under consideration, EWT-SCA performs better than EWT-EFICA and monochannel EWT approaches. But except for the frequency band below 4 Hz, which is affected by OAs, the PSDs of clean signals from all methods are very close to those of contaminated signals.

TABLE I
THE OBTAINED MAXIMUM PCER OF δ RHYTHMS, AMAE IN PSD, AND ASNR MEASURES FOR SIMULATED EEG RECORDS USING EWT-SCA.

EEG records	Maximum Δ ER$_\delta$	AMAE in PSD of EEG rhythms				ASNR i/p	ASNR o/p
		Theta	Alpha	Beta	Gamma		
sim1	81.08	0.11	1.8E-14	4.2E-15	6.2E-16	4.43	8.28
sim2	71.77	0.21	1.8E-14	4.7E-15	7.3E-16	5.83	7.98
sim6	94.50	0.02	3.6E-15	1.0E-15	3.0E-16	3.01	4.82
sim7	88.88	0.09	8.5E-15	8.8E-16	1.3E-16	3.17	5.80
sim9	95.84	0.029	1.5E-15	7.1E-16	2.1E-16	0.94	4.12
sim11	94.17	0.03	3.0E-15	8.2E-16	2.4E-16	2.39	3.72
sim12	94.27	0.05	2.2E-15	5.6E-16	1.7E-16	2.51	5.88
sim14	95.00	0.01	1.5E-15	6.8E-16	1.4E-16	1.61	4.36
sim16	88.02	0.30	1.2E-14	1.4E-15	1.7E-16	3.80	5.77
sim18	90.60	0.07	5.5E-15	1.1E-15	2.5E-16	2.82	5.74
sim20	84.39	0.19	5.3E-15	1.5E-15	2.4E-16	4.22	6.25
sim22	87.95	0.07	4.5E-15	1.2E-15	4.0E-16	4.19	5.09
sim25	93.20	0.05	3.5E-15	6.4E-16	1.5E-16	2.75	3.39
sim26	94.94	0.05	1.4E-15	3.9E-16	1.2E-16	1.85	5.33
sim28	82.95	0.11	1.3E-14	1.2E-15	2.3E-16	5.26	5.75
sim30	95.76	0.04	2.7E-15	1.1E-15	2.4E-16	2.05	3.32
sim31	90.18	0.16	1.6E-14	1.3E-15	1.8E-16	3.57	5.81
sim32	91.24	0.22	3.4E-15	1.3E-15	3.1E-16	4.11	5.53
sim34	93.82	0.13	2.5E-15	8.0E-16	2.5E-16	2.54	4.57
sim36	93.31	0.04	2.1E-15	6.1E-16	1.4E-16	2.60	4.84
sim37	93.73	0.02	3.3E-15	7.8E-16	2.1E-16	2.34	5.49
sim40	91.18	0.08	9.6E-15	1.5E-15	3.9E-16	2.68	5.87
sim43	86.90	0.05	3.8E-15	1.3E-15	3.3E-16	2.17	4.99
sim45	93.10	0.04	7.1E-15	6.2E-16	9.1E-17	1.45	3.61
sim46	94.55	0.13	5.7E-15	7.3E-16	1.5E-16	2.01	7.89
sim48	93.29	0.07	2.6E-15	8.7E-16	1.8E-16	0.54	4.97
sim50	95.71	0.04	2.6E-15	9.0E-16	2.8E-16	0.16	4.01
sim51	94.86	0.08	3.7E-15	7.7E-16	1.4E-16	0.42	4.30
sim53	92.35	0.05	5.1E-15	1.2E-15	2.2E-16	1.71	4.87
sim54	94.46	0.08	4.1E-15	1.3E-15	4.0E-16	2.07	4.91
Mean	91.07	0.09	5.9E-15	1.2E-15	2.5E-16	2.64	5.24
STD	5.25	0.07	4.8E-15	9.2E-16	1.4E-16	1.34	1.22

One can notice in Fig. 11 that the dictionary (corresponding to real EEG signal of Fig. 2) contains three different artifact patterns which are automatically included based on the criterion of high ER of the δ rhythms (see eqn (22)) belonging to different spatial locations.

Further, detecting the artifact components/sources after spatial filtering is an important step in the proposed methods. Fig. 12 presents the 14 components obtained after rotating the basis of δ-rhythms onto the dictionary using SCA. It can be seen that SCA components representing the common subspace of the two databases appear at the top, followed by the components which represent the subspace for uncontaminated δ-rhythms. Hence, the uncontaminated δ-rhythms can be recomposed after eliminating the first three common subspace basis vectors (artifact components, correspond to unitary singular values (eq. 20))

TABLE II
THE OBTAINED MAXIMUM PCER OF δ RHYTHMS AND AMAE IN PSD FOR OTHER RHYTHMS FOR REAL EEG RECORDS USING EWT-SCA.

EEG records	Maximum Δ ER_δ	AMAE in PSD of EEG rhythms			
		Theta	Alpha	Beta	Gamma
S001R01	94.457	1.009	2.50E-14	1.20E-14	5.07E-15
S001R04	89.442	0.903	2.12E-14	1.19E-14	5.51E-15
S001R06	94.405	0.918	2.46E-14	1.15E-14	4.51E-15
S001R08	90.973	1.060	2.39E-14	1.27E-14	5.42E-15
S001R11	95.377	1.023	3.55E-14	1.91E-14	8.87E-15
S001R13	93.733	1.211	3.91E-14	2.07E-14	9.03E-15
S002R03	86.078	0.268	1.11E-14	5.76E-15	3.70E-15
S002R05	91.925	0.497	1.52E-14	7.10E-15	3.76E-15
S002R07	91.304	0.620	1.01E-14	4.95E-15	3.32E-15
S002R10	87.546	0.160	8.93E-15	3.43E-15	2.08E-15
S002R11	85.057	0.323	1.17E-14	5.08E-15	3.77E-15
S002R12	88.553	0.167	1.01E-14	3.77E-15	2.30E-15
S006R05	91.678	0.754	3.72E-15	3.73E-15	2.50E-15
S006R09	91.831	0.553	4.32E-15	6.26E-15	4.45E-15
S008R04	92.149	0.480	1.05E-14	4.80E-15	3.09E-15
S008R13	90.881	1.502	2.31E-14	7.48E-15	4.28E-15
S009R10	96.23	0.952	3.47E-14	3.20E-14	3.57E-14
S009R12	95.307	0.974	3.61E-14	3.47E-14	3.40E-14
S015R04	82.465	1.462	4.46E-14	2.47E-14	8.86E-15
S015R10	86.075	1.057	4.79E-14	2.11E-14	5.02E-15
S019R05	90.625	1.206	1.74E-14	1.38E-14	7.88E-15
S019R06	90.722	1.474	1.75E-14	1.82E-14	1.14E-14
S019R07	92.131	1.698	2.08E-14	1.80E-14	1.10E-14
S019R08	86.661	0.818	1.98E-14	2.17E-14	1.44E-14
S035R03	84.656	0.367	7.68E-15	2.83E-15	8.80E-14
S035R05	88.724	0.541	9.04E-15	3.38E-15	8.16E-14
S035R07	90.453	0.319	9.39E-15	3.42E-15	5.84E-14
S036R07	93.668	2.084	6.62E-14	3.22E-14	1.82E-14
S036R12	93.826	2.076	6.29E-14	2.81E-14	1.31E-14
S108R07	94.901	1.823	3.03E-14	2.12E-14	1.56E-14
Mean $\pm$ STD	90.73 $\pm$ 3.575	0.943 $\pm$ 0.546	2.34E-14 $\pm$ 1.64E-14	1.39E-14 $\pm$ 9.85E-15	1.58E-14 2.23E-14

TABLE III
THE OBTAINED MAXIMUM PCER OF δ RHYTHMS AND AMAE IN PSD FOR OTHER RHYTHMS FOR REAL EEG RECORDS USING EWT-EFICA.

EEG Records	Maximum Δ ER$_\delta$	AMAE in PSD θ-rhythm	α-rhythm	β-rhythm	γ rhythm
S001R01	62.7484	17.5627	1.93E-14	1.06E-14	4.40E-15
S001R06	60.0487	14.5785	1.50E-14	7.31E-15	3.68E-15
S108R07	53.5186	8.7598	1.89E-14	1.48E-14	1.07E-14
S109R05	63.1863	25.4753	2.24E-14	1.41E-14	7.32E-15
S100R09	63.7358	12.8501	1.66E-14	9.86E-15	4.60E-15

TABLE IV
THE OBTAINED MAXIMUM PCER OF δ RHYTHMS AND MAE IN PSD FOR OTHER RHYTHMS FOR REAL EEG RECORDS USING MONOCHANNEL EWT.

EEG Records	Δ ER$_\delta$	MAE values in PSD θ-rhythm	α-rhythm	β-rhythm	γ-rhythm
S001R01	50.2009	2.13E-14	1.23E-14	5.32E-15	2.30E-15
S001R06	52.7896	1.23E-14	9.62E-15	4.35E-15	1.64E-15
S108R07	46.4577	3.05E-14	1.66E-14	2.01E-14	1.69E-14
S109R05	56.7107	1.96E-14	7.93E-15	2.82E-15	7.72E-16
S100R09	33.1268	3.32E-16	1.04E-16	5.00E-17	2.88E-17

using a diagonal gain matrix. Finally, the recovered δ-rhythms are combined with other EEG rhythms to reconstruct the OA-free multivariate signal. Fig. 13 shows the clean real multivariate EEG signal obtained using EWT-SCA method. For facilitating the interpretation and visual inspection, the eliminated artifacts (difference of raw EEG and processed EEG), on the same channels as in Fig. 13, are shown in Fig. 14.

Fig. 15 shows the scalograms [45] of a real OA-contaminated EEG channel before and after applying the EWT-SCA method. It can be noticed that eye artifacts with high energy concentration are absent in the TF image after filtering process.

Fig. 16 plots the variation of performance parameters, namely, MAE (for θ and α rhythms) and PCER for δ rhythm with dictionary cutoff frequencies. It can be observed that though PCER increases slightly, the MAE values increase significantly above 4 Hz dictionary cutoff frequency. Therefore, the dictionary cutoff frequency is fixed at 4 Hz for all the OA contaminated multichannel EEG records.

Fig. 17 exhibits the graphical variation of the performance parameters with respect to the number of eliminated artifact components for both simulated and real EEG signals. The subplots also present the performance of the method when a FIR filter bank replaces EWT. The trends of the subplots reveal that after eliminating a few components, the performance parameters converge. Hence, preserving the basic EEG information can be carried out by eliminating a minimal number of components.

A. Comparison with existing methods

We have compared our hybrid filtering methods with existing state-of-the-art OA removal methods in Table V. For effective extraction of OAs from the intrinsic mode functions obtained using EEMD, the authors in [44] replaced linear PCA with kernel PCA (kPCA), which outperformed the EEMD-PCA [27] and the wavelet-based (symlet (sym3) as a basis function) [43] methods in terms of MAE values in PSD for α rhythm.

Likewise, Maddirala *et al.* [25] proposed SSA and ANC combination for removal of OAs and compared the method's performance with DWT-ANC method proposed by Peng *et al.* [24]. The performance of SSA-ANC does not depend on the morphology of the EOG signal, and with an MAE value of 0.1671, it surpassed the DWT-ANC method. The DWT-ICA [23] and the rhythm-based algorithm [29] for removal of OA from EEG had MAE in PSD for α rhythm less than 0.1671, which suggests that these methods work better in preserving the non-contaminated EEG information. Comparison of the MAE values of the existing methods with the proposed approach substantiates that EWT-SCA excels overall. We have also compared the hybrid approaches with a monochannel EWT-based method and found that EWT-SCA has the least MAE values in PSD for α rhythm.

TABLE V
COMPARISON WITH THE EXISTING METHODS IN TERMS OF MAE VALUES.

Methods	Input	α rhythm MAE in PSD (σ)
Wavelet Sym3 [43]	Single channel	0.539 0.326
DWT-ANC [24]	Single channel	0.416 0.251
EEMD-PCA [27]	Single channel	0.669 0.504
EEMD-KPCA (Polynomial kernel of 3rd order) [44]	Single channel	0.583 0.413
SSA-ANC [25]	Single channel	0.167 0.053
DWT-ICA [23]	Multichannel	0.031 0.011
FBSEEWT-LPATV [29]	Single channel	0.029 0.020
EWT	Single channel	9.30E-15 6.08E-15
EWT-EFICA	Multichannel	1.61E-14 6.59E-15
EWT-SCA	Multichannel	2.34E-14 1.64E-14

TABLE VI
COMPARISON WITH THE CONVENTIONAL EEG EYE-BLINK ARTIFACT REMOVAL METHODS IN TERMS OF CCI MEASURE.

Electrode name	EWT-SCA	Wavelet ICA [15]	ASR [20]	ICLabel [16]	EEGdenoiseNet [30]
AF3	0.73	0.56	0.85	0.54	0.60
F7	0.84	0.63	0.69	0.65	0.67
F3	0.86	0.76	0.81	0.52	0.73
FC5	0.63	0.80	0.85	0.67	0.79
T7	0.76	0.75	0.92	0.89	0.82
P7	0.78	0.97	0.94	0.90	0.91
O1	0.85	0.91	0.84	0.96	0.92
O2	0.87	0.92	0.99	0.95	0.82
P8	0.86	0.88	0.94	0.86	0.84
T8	0.88	0.85	0.85	0.68	0.93
FC6	0.67	0.75	0.77	0.65	0.89
F4	0.94	0.78	0.80	0.52	0.80
F8	0.83	0.64	0.88	0.69	0.86
AF4	0.84	0.61	0.83	0.59	0.71

The resemblance of the reconstructed EEG channel with the raw EEG channel is further evaluated in terms of the correlation coefficient index (CCI) measure; the channel by channel results have been compared with four existing state-of-the-art methods [15], [16], [20], [30], enumerated in Table VI. The Higher the CCI is, the better the method is at preserving the EEG information. The wavelet-ICA method [15] achieved average CCI of 0.77 for real 14-channel EEG signals. Likewise, the multichannel EEG eye-blink artifact suppression method, namely, the ASR method [20], achieves average CCI value of 0.85 when studied in the real EEG signals considered in this work. The state-of-the-art ICLabel method [16] removed the EOG artifacts from real EEG data, resulting in an average CCI value of 0.72. The deep learning (DL) based long short-term memory (LSTM) model [30]

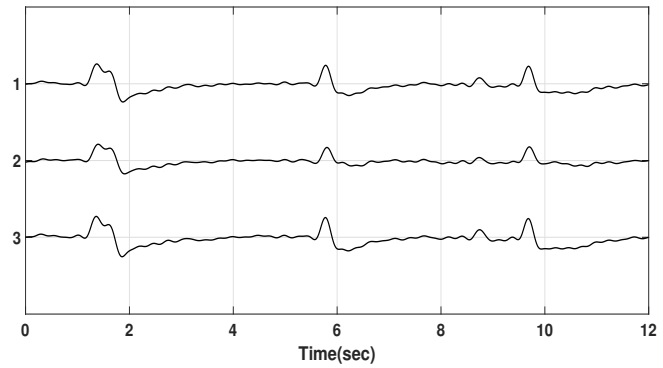

Fig. 11. Plot of the EEG artifact dictionary used for cleaning the real multichannel OA contaminated EEG signals.

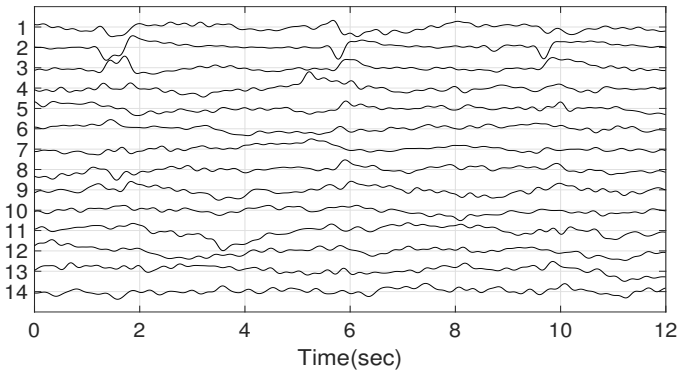

Fig. 12. Plot of the SCA components of real EEG signals contaminated with OAs.

was also tested on real EEG signals, with an average CCI value of 0.81. The DL model was trained using both clean and EOG-contaminated EEG signals available in EEGdenoiseNet [30]. Studying the real EEG signals, the average CCI value for the proposed EWT-SCA method is evaluated as 0.81, which is comparable with the existing state-of-the-art methods. Other cutting-edge EEG artifact rejection techniques exist, such as Autoreject [46], however they are not very effective for removing eye blink artifacts [46].

B. Analysis of execution time

The MATLAB platform was used to run the computer simulations on a system with an Intel(R) Core(TM) i7-8750H CPU running at 2.20 GHz and 16 GB of RAM. The proposed method takes 960 milliseconds for processing 64-channel EEG of duration 125 s. As can be seen in Fig. 18, the proposed method executes much faster than the traditional ASR method [20] for several real-world EEG sessions. On the other hand, the wavelet ICA method [15] has a mean execution time of 0.060 s for processing 12 channel EEG signal of 105 s duration.

C. Discussion

The proposed methodology uses the capabilities of EWT-based frequency filtering and spatial filtering techniques and presents a new enhanced hybrid approach. Building an artifact-rich dictionary is a crucial step in SCA based approach.

In a nutshell, we seek to eliminate or reduce the eye artifacts on surface EEG signals using a dictionary based approach that can be seen as a non-linear spatial filter in three steps: (1) we extract the dictionary from the raw data by EWT and channel selection; (2) we transform the raw data by spatial filtering (i.e. by rotating its basis onto the artifact space basis), the result being to identify artifact basis signals; (3) the signals constituting the artifact basis are zeroed before the final reconstruction step, which yields clean EEG signals. Our method, in contrast to existing ones, derives the artifact basis dictionary from the raw data itself rather than using reference signals like EOG. It is more flexible than fixed reference signals since it serves as the basis of the artifact space (it allows reconstructing different versions of the artifacts). One can argue that this technique is also used by BSS/ICA based methods. Still, a key difference with these approaches is the use of the (physiologically meaningful) dictionary to optimize the rotation of the signal space basis (while in ICA, the rotation maximises the independence, with no particular concern about the physiological plausibility of the extracted basis of independent “sources”).

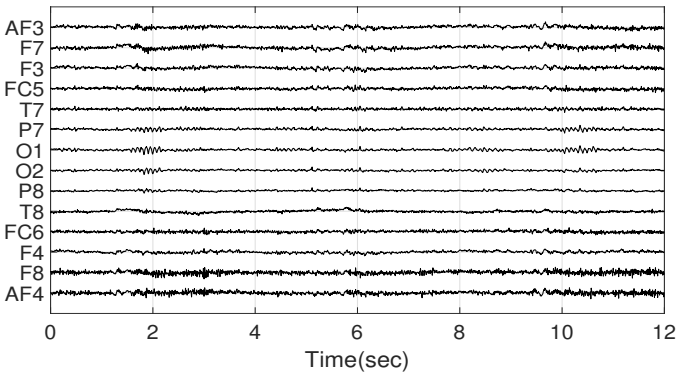

Fig. 13. Plot of the OA-free real multichannel EEG signals obtained using EWT-SCA.

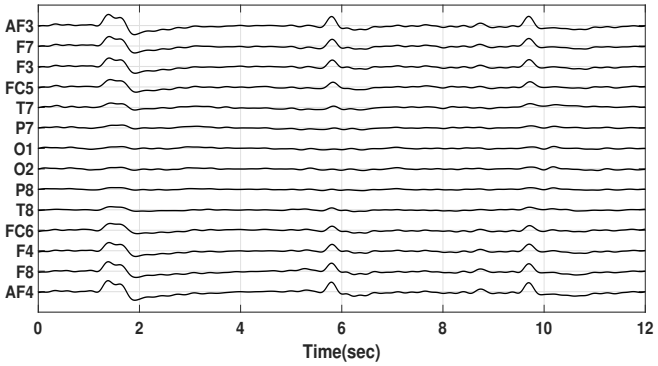

Fig. 14. Plot of the channel-wise eliminated OAs using EWT-SCA method.

As mentioned above, BSS methods decompose the data and could be in principle used to construct an artifact dictionary [16], [17], but identifying the artifact sources is challenging and more subjective as they appear randomly after the demixing process and, moreover, they could be mixed among them or even with brain sources.

The proposed method is fast and reliable and has been proven successful in removing artifacts from multichannel EEG signals recorded for brain-computer interface (BCI) applications, showing performances similar or better than state of the art algorithms [16], [20], [30]. Other applications can be explored, such as the removal of cardiac artifacts from multichannel EEG signals with the help of a dictionary constructed with multi-lead ECG signal recordings that are generally used for cardiac screening [47].

One should mention nevertheless that the method assumes that high amplitude δ waves are mostly eye artifacts (which is a common assumption in in the awake state and thus in BCI applications). If this condition is not fulfilled the design of the dictionary should be revisited. More generally, the method is sensitive to the choice of the artifact dictionary/basis, which should be chosen carefully (see analysis of the cutoff frequency, figure 16).

Evaluating the BCI performance after applying the proposed method would be an important issue, but this is beyond the scope of the work reported here and will be left for further research. One can indeed note that ERPs used in BCI (such as P300 for example) are also low frequency events [48], so one might wonder if they would be affected by the denoising procedure. Although not evaluated, as stated above, we conjecture that they will not be cancelled, because they will not belong to the dictionary used for spatial filtering, as they will not belong to channels with high ER in the δ band (P300 ERPs are low amplitude events that become visible only after averaging over several occurrences.) More generally, comparisions of BCI performances (ERP detection and/or classification, but also the effect on frequency based methods for steady-state BCI approaches) is an important task which deserves a complete study in our opinion. Besides the preprocessing, the results will certainly depend on the task, as well as on the BCI specific algorithms.

It is noteworthy that the cancellation of eye artifacts proposed here, as any preprocessing methods, influences all further signal processing steps and the outcome of further analysis. Besides BCI, another important example is the estimation of functional connectivity, useful for clinical diagnostics (see e.g. [49]). We believe that the method we propose here, while eliminating spurious connectivity measures due to eye artifacts, will not distort the estimation of important physiological connectivity measures, as it only affects limited frequency bands.

Finally, we can also note that, while the proposed method is designed for ocular artifact cancelling only, it can be used to

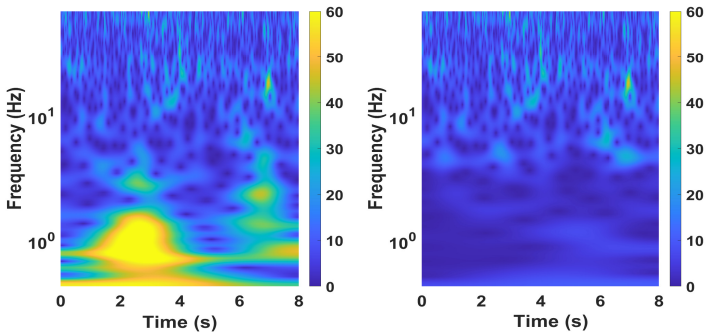

Fig. 15. Plots of scalograms of a OA contaminated (real) EEG channel before (left) and after (right) applying EWT-SCA.

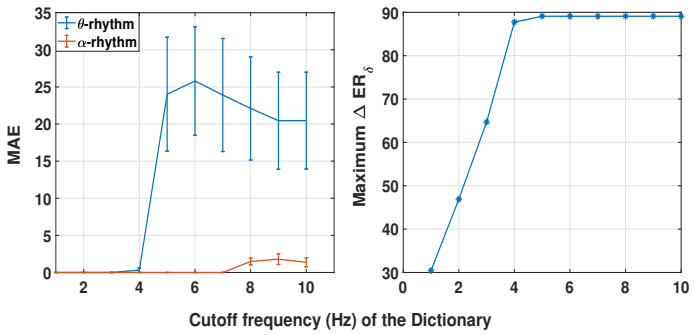

Fig. 16. Plots of the variation of performance parameters with dictionary cutoff frequencies.

complement other artifact cancellation techniques (similar to other methods, see [20]). The MATLAB code of the proposed EWT-SCA based OA removal method is available at the following link: https://github.com/abhijit12345678910/EOG-artifact-removal-from-multichannel-EEG-signals.

V. Conclusion

We have proposed various combinations of frequency and spatial filtering techniques to remove ocular artifacts (OAs) from multichannel EEG signals in the awake state. The empirical wavelet transform (EWT), which is the initial step in the proposed method, is used to decompose EEG signals into rhythms. As OAs mostly contaminate the low-frequency range of the EEG signals, the δ-rhythms have been further considered for spatial filtering. The spatial filtering technique, namely subspace correlation approach (SCA) armed with an artifact-rich dictionary (containing filtered artifact patterns from different spatial locations), has been optimally utilized to separate the OAs and neural information in the δ-rhythms. Finally, the artifact components have been eliminated before inverse spatial filtering and cleaned δ-rhythms are combined with other frequency bands of the EEG signals. While the SCA spatial filtering embeds *a priori* knowledge on the nature of the artifacts, blind methods can also be used. We have in particular tested a blind source separation method, EFICA, for separating the artifact and neural sources. EWT-SCA performed the best in removing the OAs and preserving the EEG information out of all the proposed hybrid methods. Furthermore, the complete filtering procedure has been automated without any supplementary reference signals and can be employed in real-time to clean a large EEG dataset contaminated with OAs.

To conclude, we might note that, even if the performances of our method were clearly demonstrated on the publicly available dataset [35], further research is needed to validate it on other datasets, as for example clinical signals recorded in the context of different pathologies (epilepsy, Alzheimer, etc). As mentioned previously in the Discussion, another future research direction is the study of the influence of our method on the performances of further processing tasks such as BCI or connectivity analysis.

References

[1] A. Q. Rana, A. T. Ghouse, and R. Govindarajan, *Basics of Electroencephalography (EEG)*. Cham: Springer International Publishing, 2017, pp. 3–9.
[2] M. Teplan *et al.*, "Fundamentals of EEG measurement," *Measurement science review*, vol. 2, no. 2, pp. 1–11, 2002.
[3] A. Bhattacharyya and R. B. Pachori, "A multivariate approach for patient-specific EEG seizure detection using empirical wavelet transform," *IEEE Transactions on Biomedical Engineering*, vol. 64, no. 9, pp. 2003–2015, 2017.
[4] Y. Kang *et al.*, "Principal dynamic mode analysis of EEG data for assisting the diagnosis of alzheimers disease," *IEEE Journal of Translational Engineering in Health and Medicine*, vol. 3, pp. 1–10, 2015.

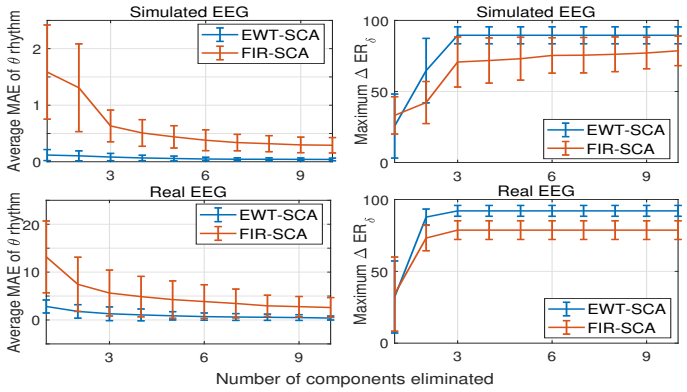

Fig. 17. Plots of AMAE_θ and Maximum Δ ER_δ versus the number of eliminated components for simulated and real multichannel EEG signals.

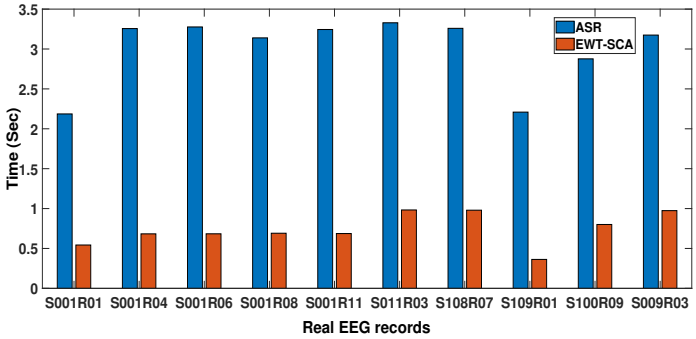

Fig. 18. Plot of the execution times of the proposed EWT-SCA method and state-of-the-art ASR method for cleaning different real EEG sessions.

[5] A. Bhattacharyya *et al.*, "A multi-channel approach for cortical stimulation artefact suppression in depth EEG signals using time-frequency and spatial filtering," *IEEE Transactions on Biomedical Engineering*, vol. 66, no. 7, pp. 1915–1926, 2019.

[6] A. Liu *et al.*, "Muscle artifact removal towards mobile SSVEP-based BCI: A comparative study," *IEEE Transactions on Instrumentation and Measurement*, 2021.

[7] K. T. Sweeney, T. E. Ward, and S. F. McLoone, "Artifact removal in physiological signalspractices and possibilities," *IEEE Transactions on Information Technology in Biomedicine*, vol. 16, no. 3, pp. 488–500, 2012.

[8] W. Barry and G. Jones, "Influence of eye lid movement upon electro-oculographic recording of vertical eye movements," *Aerospace medicine*, vol. 36, p. 855858, September 1965.

[9] M. Iwasaki *et al.*, "Effects of eyelid closure, blinks, and eye movements on the electroencephalogram," *Clinical Neurophysiology*, vol. 116, no. 4, pp. 878–885, 2005.

[10] G. L. Wallstrom *et al.*, "Automatic correction of ocular artifacts in the EEG: a comparison of regression-based and component-based methods," *International Journal of Psychophysiology*, vol. 53, no. 2, pp. 105–119, 2004.

[11] S. Romero, M. A. Maanas, and M. J. Barbanoj, "Ocular reduction in EEG signals based on adaptive filtering, regression and blind source separation," *Annals of Biomedical Engineering*, vol. 37, no. 1, pp. 176–191, Jan. 2009.

[12] P. He, G. Wilson, and C. Russell, "Removal of ocular artifacts from electro-encephalogram by adaptive filtering," *Medical and Biological Engineering and Computing*, vol. 42, no. 3, pp. 407–412, May 2004.

[13] A. Flexer *et al.*, "Using ICA for removal of ocular artifacts in EEG recorded from blind subjects," *Neural Networks*, vol. 18, no. 7, pp. 998–1005, 2005.

[14] A. K. Maddirala and R. A. Shaik, "Separation of sources from single-channel EEG signals using Independent Component Analysis," *IEEE Transactions on Instrumentation and Measurement*, vol. 67, no. 2, pp. 382–393, 2018.

[15] R. Mahajan and B. I. Morshed, "Unsupervised eye blink artifact denoising of EEG data with modified multiscale sample entropy, kurtosis, and wavelet-ICA," *IEEE Journal of Biomedical and Health Informatics*, vol. 19, no. 1, pp. 158–165, 2014.

[16] L. Pion-Tonachini, K. Kreutz-Delgado, and S. Makeig, "ICLabel: An automated electroencephalographic independent component classifier, dataset, and website," *NeuroImage*, vol. 198, pp. 181–197, 2019.

[17] R. Romo Vzquez *et al.*, "Blind source separation, wavelet denoising and discriminant analysis for EEG artefacts and noise cancelling," *Biomedical Signal Processing and Control*, vol. 7, no. 4, pp. 389–400, 2012.

[18] T. . Jung *et al.*, "Removing electroencephalographic artifacts: comparison between ICA and PCA," in *Neural Networks for Signal Processing VIII. Proceedings of the 1998 IEEE Signal Processing Society Workshop (Cat. No.98TH8378)*, 1998, pp. 63–72.

[19] C. A. E. Kothe and T.-P. Jung, "Artifact removal techniques with signal reconstruction," Apr. 28 2016, US Patent App. 14/895,440.

[20] C.-Y. Chang *et al.*, "Evaluation of artifact subspace reconstruction for automatic artifact components removal in multi-channel EEG recordings," *IEEE Transactions on Biomedical Engineering*, vol. 67, no. 4, pp. 1114–1121, 2019.

[21] T. Zikov *et al.*, "A wavelet based de-noising technique for ocular artifact correction of the electroencephalogram," in *Proceedings of the Second Joint 24th Annual Conference and the Annual Fall Meeting of the Biomedical Engineering Society] [Engineering in Medicine and Biology*, vol. 1, 2002, pp. 98–105 vol.1.

[22] S. Khatun, R. Mahajan, and B. I. Morshed, "Comparative study of wavelet-based unsupervised ocular artifact removal techniques for single-channel EEG data," *IEEE Journal of Translational Engineering in Health and Medicine*, vol. 4, pp. 1–8, 2016.

[23] M. T. Akhtar, W. Mitsuhashi, and C. J. James, "Employing spatially constrained ICA and wavelet denoising, for automatic removal of artifacts from multichannel EEG data," *Signal Processing*, vol. 92, no. 2, pp. 401–416, 2012.

[24] H. Peng *et al.*, "Removal of ocular artifacts in EEGan improved approach combining DWT and ANC for portable applications," *IEEE Journal of Biomedical and Health Informatics*, vol. 17, no. 3, pp. 600–607, 2013.

[25] A. K. Maddirala and R. A. Shaik, "Removal of EOG artifacts from single channel eeg signals using combined singular spectrum analysis and adaptive noise canceler," *IEEE Sensors Journal*, vol. 16, no. 23, pp. 8279–8287, 2016.

[26] A. Egambaram *et al.*, "FastEMDCCA algorithm for unsupervised and fast removal of eyeblink artifacts from electroencephalogram," *Biomedical Signal Processing and Control*, vol. 57, p. 101692, 2020.

[27] R. Patel *et al.*, "Ocular artifact suppression from EEG using ensemble empirical mode decomposition with principal component analysis," *Computers & Electrical Engineering*, vol. 54, pp. 78–86, 2016.

[28] M. Saini, Payal, and U. Satija, "An effective and robust framework for ocular artifact removal from single-channel EEG signal based on variational mode decomposition," *IEEE Sensors Journal*, vol. 20, no. 1, pp. 369–376, Jan. 2020.

[29] P. Gajbhiye, R. K. Tripathy, and R. B. Pachori, "Elimination of ocular artifacts from single channel EEG signals using FBSE-EWT based rhythms," *IEEE Sensors Journal*, vol. 20, no. 7, pp. 3687–3696, 2020.

[30] H. Zhang *et al.*, "EEGdenoiseNet: a benchmark dataset for deep learning solutions of EEG denoising," *Journal of Neural Engineering*, vol. 18, no. 5, p. 056057, 2021.

[31] G. H. Golub and C. F. Van Loan, *Matrix Computations, vol. 3*. John Hopkins University Press, Baltimore, MA, 2012.

[32] J. Gilles, "Empirical wavelet transform," *IEEE Transactions on Signal Processing*, vol. 61, no. 16, pp. 3999–4010, 2013.

[33] M. A. Klados and P. D. Bamidis, "A semi-simulated EEG/EOG dataset for the comparison of EOG artifact rejection techniques," *Data in Brief*, vol. 8, pp. 1004–1006, 2016.

[34] G. Schalk *et al.*, "BCI2000: a general-purpose brain-computer interface (BCI) system," *IEEE Transactions on Biomedical Engineering*, vol. 51, no. 6, pp. 1034–1043, 2004.

[35] A. L. Goldberger *et al.*, "PhysioBank, PhysioToolkit, and PhysioNet," *Circulation*, vol. 101, pp. e215–e220, Jun. 2000.

[36] A. Bhattacharyya *et al.*, "A novel approach for automated detection of focal EEG signals using empirical wavelet transform," *Neural Computing and Applications*, vol. 29, no. 8, pp. 47–57, Apr. 2018.

[37] I. Daubechies, *Ten Lectures on Wavelets*, ser. CBMS-NSF Regional Conference Series in Applied Mathematics. Society for Industrial and Applied Mathematics, Jan. 1992.

[38] R. Ranta *et al.*, "Approximate canonical correlation analysis for common/specific subspace decompositions," *Biomedical Signal Processing and Control*, vol. 68, p. 102780, 2021.

[39] A. Cichocki and S.-i. Amari, *Adaptive blind signal and image processing: learning algorithms and applications*. John Wiley & Sons, 2002.

[40] A. Hyvarinen, "Fast and robust fixed-point algorithms for independent component analysis," *IEEE Transactions on Neural Networks*, vol. 10, pp. 626–634, May 1999.

[41] A. Belouchrani *et al.*, "A blind source separation technique using second-order statistics," *IEEE Transactions on Signal Processing*, vol. 45, pp. 434–444, Feb. 1997.

[42] P. Tichavsk *et al.*, "Blind signal separation by combining two ICA algorithms: HOS-based EFICA and time structure-based WASOBI," in *2006 14th European Signal Processing Conference*, Sep. 2006, pp. 1–5.

[43] W.-Y. Hsu *et al.*, "Wavelet-based envelope features with automatic EOG artifact removal: Application to single-trial EEG data," *Expert Systems with Applications*, vol. 39, no. 3, pp. 2743–2749, 2012.

[44] R. Patel, K. Gireesan, and S. Sengottuvel, "Decoding non-linearity for effective extraction of the eye-blink artifact pattern from EEG recordings," *Pattern Recognition Letters*, vol. 139, pp. 42–49, 2020.

[45] J. M. Lilly and S. C. Olhede, "Higher-order properties of analytic wavelets," *IEEE Transactions on Signal Processing*, vol. 57, no. 1, pp. 146–160, 2008.

[46] M. Jas *et al.*, "Autoreject: Automated artifact rejection for MEG and EEG data," *NeuroImage*, vol. 159, pp. 417–429, 2017.

[47] P. Hao *et al.*, "Multi-branch fusion network for Myocardial infarction screening from 12-lead ECG images," *Computer Methods and Programs in Biomedicine*, vol. 184, p. 105286, 2020.

[48] L. Bougrain, C. Saavedra, and R. Ranta, "Finally, what is the best filter for P300 detection?" in *TOBI Workshop lll- Tools for Brain-Computer Interaction - 2012*, Würzburg, Allemagne, Mar. 2012, iPS IPS.

[49] H. Vlez-Prez *et al.*, "EEG preprocessing for synchronization estimation and epilepsy lateralization," in *2011 Annual International Conference of the IEEE Engineering in Medicine and Biology Society*, 2011, pp. 5028–5031.